Proceedings of COBEM 2005
18th International Congress of Mechanical Engineering
November 6-11, 2005, Ouro Preto, MG

ON THE UNSTEADY MOTION OF AN ISOLATED SEDIMENTING PARTICLE

Yuri Dumaresq Sobral
Department of Applied Mathematics and Theoretical Physics, University of Cambridge. Centre for Mathematical Sciences, Wilberforce Road, Cambridge, CB3 0WA, United Kingdom
e-mail: Y.D.Sobral@damtp.cam.ac.uk

Francisco Ricardo Cunha, (corresponding author)
Departamento de Engenharia Mecânica, Universidade de Brasília. Campus Universitário Darcy Ribeiro, 70910-900 Brasília - DF, Brazil.
e-mail: frcunha@unb.br

Abstract. *We consider the unsteady motion of a sedimentating rigid spherical particle in order to examine the relative strength of the hydrodynamical forces acting on particles in fluid flows. The relative strength of the forces on all stages of the particle motion is a major concern for closuring constitutive equations describing the more complex motion of particulate flows such as fluidized beds. At the regime of low particle Reynolds number, a linear viscous force, a weak non-linear inertial correction force, an added mass force and a memory force are considered. Individual expressions for these forces are proposed based on analytical solutions of the flow past a sphere at different limiting cases. The resulting model is then represented by a first order non-linear integro-differential equation in terms of the instantaneous velocity of the sphere. This equation is made dimensionless and the particle Reynolds number and the fluid-particle density ratio are identified as the relevant physical parameters for describing the particle motion. We obtain exact solutions for the limits of small density ratios and zero Reynolds number and an asymptotic solution for small density ratios and small Reynolds number. In addition, a numerical solution is used for arbitrary values of the density ratio and Reynolds number, the latter being still small but not null. The results show that the motion of spherical particles is significantly affected by the unsteady drag dominated by the memory Basset force at the early stages of the motion and on the approach to the steady state (terminal velocity). The motion is also disturbed by the non-linear inertial drag correction on the mid-time approach to steady state for moderate density ratios (say, order 1). However, for density ratios much smaller than unity, only negligible changes on the late approach to steady state are observed. These results indicate that the unsteady and convective inertial hydrodynamic drags might become of the same order of magnitude of the dominate viscous drag for flows with moderate particle-fluid density ratio. Such contributions should be taken into account on modelling multiphase particulate flows with similar density ratio.*

Keywords: *sedimentation, hydrodynamic drag, Oseen correction, Virtual mass, Basset drag*

1. Introduction

The correct prediction of the dynamics of particulate flows is of major importance in fluid mechanics. In general, this problem involves several particles with non-negligible inertia in flows with important relative velocities between the fluid and the particles, and therefore are treated as two fluids problem for which there is an interaction force term that needs to be modeled (e.g. Anderson & Jackson, 1967). This interaction force represents the interactions between the fluid and the set of particles that compose the particulate flow. A more complete model for this term should consider the full physical mechanisms of interaction between the fluid and the particle. In this work, we investigate the motion of one isolated particle sedimentating in a fluid in order to identify and evaluate the relevant mechanisms of interactions that should be considered in continuum models of particulate flows.

G.G. Stokes (cf. Batchelor, 1967) addressed the motion of an isolated sedimenting particle in a fluid for the case where the inertia of the flow was negligible, the flow field being totally dominated by viscous diffusion. This assumption, however, fails in the regions far from the particle, even for very slow motions, as shown by Oseen (cf. Batchelor, 1967). When small amounts of inertia are considered in the far region of the particle by the means of Oseen's approximation (cf. Batchelor, 1967), the solution of the flow field is no longer symmetrical, and a wake region where convection of vorticity becomes an important transport mechanism is observed. As a result of this, a non-linear (small) correction in terms of the particle velocity is obtained for the total drag on the particle. Basset (1888), on the other hand, found a solution to the linear problem with the non-linear terms of the Navier-Stokes equation being neglected. Basset identified also a memory-like contribution to the drag on particle, which depends on the history of the motion of the particle and on the viscosity of the flow. This represents a coupling of the inertial and diffusive mechanisms responsible for changing the transport of vorticity in the flow. Nevertheless, as a consequence of the non-linearity of the Navier-Stokes equation, the coupling of the non-linear inertial effects on the wakes of the particles with the transient history-dependent diffusion of vorticity is not simply additive (Lovalenti & Brady, 1993). In fact, the inertia is responsible for significant changes on the evolution of the motion of the particle. It is observed that the decay of resultant force acting on the particle when it approaches the steady state changes from $t^{-1/2}$ to t^{-2}.

Some works have been concerned about analytical solutions of the equations of motion and whether their solutions are able to reproduce the change in the temporal decay of the resultant force on the particle. Sano (1981) obtained an elegant $\mathcal{O}(Re^2 \ln(Re))$ solution for the drag acting on a spherical particle based on a multiscale asymptotic analysis of the impulsive motion of the particle and his solution revealed the change of order in time above mentioned. Lovalenti & Brady (1993) treated the same problem using the

reciprocity theorem (Kim & Karilla, 1991) to solve directly the force acting on the particle and obtained several orders of decay in time, such as t^{-1}, $t^{-5/2}\exp(-t)$, $t^{-2}\exp(-t)$, as well as $t^{-1/2}$ and t^{-2}, depending on the initial conditions of the problem. Lawrence & Mei (1995) were concerned with the long time behavior of impulsive motions of particles in fluids. In their work, they have used a modified convolution kernel for the history-dependent drag on the particle in order able to obtain the correct temporal decays of the resultant force acting on the particle. Coimbra & Rangel (1998) developed a solution for the equation of motion of the particle, which were non-linear due to the presence of relative accelerations written in terms of material derivatives. By solving the problem for previously know flow fields, the non-linearities were converted into inhomogeneities in the governing equations. The use of the Sturm-Liouville fractional derivatives allowed the authors to obtain a closed solution to the drag acting on the particle. This work, however, was unable to recover the correct temporal decays of the resultant force on the particle because of the use of the traditional kernel for the history-dependent drag on the particle.

The aim of the present work is three-fold. Firstly, we want propose a simple model for the motion of the particle and obtain analytical and numerical solutions for all limiting regimes of the flow that are consistent with the model. Secondly, based on our simple model, we investigate the time evolution of the particle motion towards the steady state in order to determine the relevant forces acting on the particle and in which stages of the particle motion this happens. This may indicate the relevant forces that should be considered in modeling fluid-particle interaction force in continuum formulations of particulate flow problems. Finally, we study the coupling of the inertial and the history-dependent drags in order to determine whether the model explored here is able to reproduce the temporal decays observed in the experiment of the unsteady hydrodynamic force exerted on an isolated sedimenting particle.

2. The governing equation

The equation of motion of the particle is obtained from the Newton's second law, that is,

$$\sum \mathbf{F} = m_p \frac{d\hat{\mathbf{v}}}{d\hat{t}}, \tag{1}$$

where $\mathbf{F}$ denotes the forces that are acting on the particle, m_p is the mass of the particle and $d\hat{\mathbf{v}}/d\hat{t}$ its acceleration. Therefore, it is needed to identify the hydrodynamic and non-hydrodynamic forces acting on the particle in order to solve Eq.(1). Some of the modeled forces are evaluated by scaling arguments based on the Navier-Stokes equation for a incompressible fluid flow, namely

$$\rho_f \left(\frac{\partial \hat{\mathbf{u}}}{\partial \hat{t}} + \hat{\mathbf{u}} \cdot \nabla \hat{\mathbf{u}} \right) = -\nabla \tilde{p} + \mu_f \nabla^2 \hat{\mathbf{u}} + \rho_f \mathbf{g}, \tag{2}$$

where $\hat{\mathbf{u}}$ is the fluid velocity, ρ_f and μ_f denote the fluid density and the dynamical viscosity, respectively, $\tilde{p}$ is the pressure on the fluid and $\mathbf{g}$ is the local gravitational acceleration. For instance note that all these quantities are dimensional.

Balancing the pressure and the viscous terms in Eq.(2), it can be seen that there should be a force f_μ, linear in terms of the particle velocity, that scales with $f_\mu \sim \mu_f L U$, where L and U are scales for length and velocity of the particle, respectively. If the non-linear inertial term is balanced with the pressure term instead, then there should also be a force f_ρ that scales as $f_\rho \sim \rho_f L^2 U^2$, which is found to be non-linear in terms of the particle velocity. Repeating the same procedure with the transient inertial term, a force $f_{mv} \sim \rho_f L^3 U/\tau_p$ is found to be depend upon a time scale τ_p, denoting the typical time scale of the motion of the particle.

In addition to the hydrodynamic forces discussed above, the force corresponding to the net weight on the particle is expressed by

$$\mathbf{f}_g = \vartheta_p(\rho_p - \rho_f)\mathbf{g} = \vartheta_p \Delta\rho \mathbf{g}, \tag{3}$$

which is the force that actually drives the particle settling. In Eq.(3), ϑ_p denotes the volume of the particle and ρ_p represents its density. We also consider a "memory-like" force, the Basset drag f_b, that will be discussed later. Therefore, the equation of motion of a spherical particle in sedimentation can be written as

$$\mathbf{f}_\mu + \mathbf{f}_\rho + \mathbf{f}_{vm} + \mathbf{f}_b + \mathbf{f}_g = m_p \frac{d\hat{\mathbf{v}}}{d\hat{t}}, \tag{4}$$

where all the terms on the left hand side on equation (4) are vectorial quantities. Despite the fact that the scales of some of these forces are known, the precise relations for each of them need to be proposed.

An expression for the force $\mathbf{f}_\mu$ can be obtained from the analytical solution of Eq.(2) when the inertia of the flow (both the transient and the convective inertia) is completely neglected and only the viscous diffusion of vorticity governs the motion of the fluid. This corresponds to the well know Stokes's solution for viscous drag force (Batchelor, 1967) of the flow past a sphere given by

$$\mathbf{f}_\mu = 6\pi\mu_f a \hat{\mathbf{v}}, \tag{5}$$

where $\hat{\mathbf{v}}$ is the instantaneous velocity of the particle. When the drag obtained in Eq.(5) is balanced with the net weight of the particle, the terminal velocity of the particle is obtained to be

$$U_s = \frac{9}{2}\frac{a^2 \Delta\rho \mathrm{g}}{\mu_f}. \tag{6}$$

It should be important to note that neglecting the transient part of the flow inertia does not imply that the flow is steady. It means that the forces on the fluid are in dynamical equilibrium, this equilibrium happening in a time scale much shorter than the time scale in

which the particle motion is developed. Therefore, the instantaneous structure of the flow depends on the boundary conditions of the problem only. In this case, the flow (and the force acting on the particle) is said to be quasi-steady.

Stokes' solution, however, exhibits physical inconsistence in the region far from the sphere, when the inertia of the flow is very small, but not negligible (Batchelor, 1967). Consider that the scale of the velocity induced on the flow by the motion of the particle at a distance r from its center is $U_r \sim U_t a/r$. From Eq.(2), it can be obtained that the viscous terms scale as $\mid \mu_f \nabla^2 \hat{\mathbf{u}} \mid \sim \mu_f U a/r^3$. Far from the particle, the inertia term $\partial \hat{\mathbf{u}}/\partial \hat{t}$ in Eq.(2) can be identified with $-\hat{\mathbf{v}} \cdot \nabla \hat{\mathbf{u}}$. This term scales as $\mid \rho_f \hat{\mathbf{v}} \cdot \nabla \hat{\mathbf{u}} \mid \sim \rho_f a U_t^2/r^2$, and taking the ratio between this scale and the scale for the viscous terms, its is verified that the inertia can be neglected on the flow when $Re_* r/a \ll 1$, where $Re_* = \rho_f a U_t/\mu_f$. Therefore, on the region far from the sphere, $r > a/Re_*$ the Stokes' approximation is no longer valid and inertia cannot be neglected. The Oseen approximation leads to a problem that can be solved analytically for small Re_* limits (Batchelor, 1967). The solution to the drag acting on the particle has, besides the linear Stokes drag, a small non-linear correction that we identify as being $\mathbf{f}_\rho$, that is,

$$\mathbf{f}_\rho = \frac{9}{4}\pi a^2 \rho_f \hat{\mathbf{v}} |\hat{\mathbf{v}}|. \tag{7}$$

The unsteady force f_{vm} is associated to the inertia of the fluid surrounding the particle. This is called the virtual mass drag and can be calculated from the potential flow past a sphere (Batchelor, 1967), namely

$$\mathbf{f_{mv}} = \frac{2}{3}\pi a^3 \rho_f \frac{d\hat{\mathbf{v}}}{d\hat{t}}. \tag{8}$$

Note that the coefficient of the time derivative in Eq.(8) is the mass of fluid associated with the half of the volume of the sphere, corresponding to the virtual mass of fluid accelerated by the particle.

Now, we gives the expression for the force $\mathbf{f}_b$. Basset (1888) developed an analytical solution of Eq.(2) for the case in which the non-linear term $\rho_f \hat{\mathbf{u}} \cdot \nabla \hat{\mathbf{u}}$ is neglected. This problem can be solved by the means of spherical harmonics or by Fourier transforms (Landau & Lifschitz, 1971), and the solution to the hydrodynamic force on the sphere yields the Stokes drag, the virtual mass drag and an extra unsteady force given by following convolution integral

$$\mathbf{f}_b = 6a^2\sqrt{\pi \rho_f \mu_f} \int_o^{\hat{t}} \left(\frac{d\hat{\mathrm{v}}}{d\hat{t}}\right)_{\hat{t}=\zeta} \frac{1}{\sqrt{\hat{t}-\zeta}} d\zeta, \tag{9}$$

where ζ is an integration variable. This term couples the history of the acceleration of the particle with the viscosity of the fluid, indicating a transient diffusion of vorticity in the flow. In fact, the coefficients of the Basset in Eq.(9) may be re-written in terms of the Stokes drag in Eq.(5) and that of the virtual mass drag in Eq.(8) as follows

$$a^2\sqrt{\rho_f \mu_f} = \sqrt{(\mu_f a)\,(\rho_f a^3)}, \tag{10}$$

So, the coefficient of the Basset force corresponds to the geometric mean between the viscous drag coefficient and the virtual mass drag coefficient.

Now, we consider the 1D version of Eq.(4) adopting the positive sense of motion downwards. By this convection the drag forces that resist the motion of the particle are negative forces. We obtain

$$\begin{aligned} m_p \frac{d\hat{\mathrm{v}}}{d\hat{t}} &= -6\pi\mu_f a\hat{\mathrm{v}} - \frac{9}{4}\pi\rho_f a^2 \hat{\mathrm{v}}^2 - \frac{2}{3}\pi\rho_f a^3 \frac{d\hat{\mathrm{v}}}{d\hat{t}} \\ &- 6a^2\sqrt{\pi\rho_f\mu_f} \int_o^{\hat{t}} \left(\frac{d\hat{\mathrm{v}}}{d\hat{t}}\right)_{\hat{t}=\zeta} \frac{1}{\sqrt{\hat{t}-\zeta}} d\zeta + \vartheta_p(\rho_p - \rho_f)\mathrm{g}, \end{aligned} \tag{11}$$

where $\hat{\mathrm{v}}$ and g is the gravity.

Eq.(11) can be made non-dimensional by choosing the terminal Stokes velocity U_s in Eq.(6) and the particle relaxation time $\tau_r = m_p/(6\pi\mu_f a)$, as the characteristic velocity and time scales, respectively. Defining the dimensionless variables $\mathrm{v} = \hat{\mathrm{v}}/U_s$ and $t = \hat{t}/\tau_r$, Eq.(11) can be written in a non-dimensional form as

$$\left(1 + \frac{1}{2}\chi\right)\frac{d\mathrm{v}}{dt} + \mathrm{v} + \frac{3}{8}Re_s\mathrm{v}^2 + \sqrt{\frac{9\chi}{2\pi}} \int_o^t \left(\frac{d\mathrm{v}}{dt}\right)_{t=\zeta} \frac{1}{\sqrt{t-\zeta}} d\zeta - 1 = 0. \tag{12}$$

In the above equation, it is identified two relevant physical parameters governing the particle motion; the density ratio $\chi = \rho_f/\rho_p$ and the Reynolds number based on the Stokes terminal velocity, $Re_s = (\rho_f a U_s)/\mu_f$. It should be noted that if the terminal velocity of the particle U_t had been chosen as a velocity scale, in Eq.(12) instead of U_s we would find, in addition to the Reynolds number and the density ratio, the sedimentation number $N_s = U_s/U_t$. Eq.(12) is an integro-differential non-linear first order differential equation and is associated to the initial condition

$$\mathrm{v}(0) = 0. \tag{13}$$

The solution of Eq.(12) and Eq.(13) gives the motion of the particle as a function of time. As we will discuss later, it has not been obtained yet an analytical solution to Eq.(12) in its complete form. Some particular cases, however, can be solved analytically and allowing a precise analysis of each individual mechanism (or force) that were added to the present model.

3. Analytical solutions of the governing equation

3.1. Linear equation

the simplest form of equation (12), corresponds to the case in which only the viscous and the virtual mass forces are considered in addition to the net weight of the particles. In this case, Eq.(12) reduces to

$$\left(1+\frac{1}{2}\chi\right)\frac{d\mathrm{v}}{dt}+\mathrm{v}-1=0, \tag{14}$$

that admits direct integration. For this simple case the velocity of the particle is simply given by

$$\mathrm{v}(t)=1-\exp\left(-\frac{t}{1+\frac{1}{2}\chi}\right). \tag{15}$$

3.2. Non-linear equation with no memory effects

When only the memory effects are neglected in Eq.(12), the motion of the particle is governed by the following non-linear inhomogeneous differential equation

$$\left(1+\frac{1}{2}\chi\right)\frac{d\mathrm{v}}{dt}+\mathrm{v}+\frac{3}{8}Re_s\mathrm{v}^2-1=0. \tag{16}$$

The above equation does not have an analytical exact solution. It is possible, however, to obtain an analytical approximated solution when Eq.(16) is weakly non-linear, that means for small Re_sl. Consider a small parameter ε to be defined as $\varepsilon=\frac{3}{8}Re_s$. The solution of Eq.(16) can be proposed in terms of a asymptotic expansion for $\mathrm{v}(t)$ as

$$\mathrm{v}(t)=\sum_{k=0}^{\infty}\varepsilon^k\mathrm{v}_k(t), \tag{17}$$

where the subindex k denote the k-th term of the series. We then found the asymptotic solution for the velocity of the particle up to the $\mathcal{O}(\varepsilon^4)$ terms as being

$$\mathrm{v}(t)=\mathrm{v}_o(t)+\varepsilon\mathrm{v}_1(t)+\varepsilon^2\mathrm{v}_2(t)+\varepsilon^3\mathrm{v}_3(t)+\varepsilon^4\mathrm{v}_4(t)+\mathcal{O}(\varepsilon^5), \tag{18}$$

with

$$\mathrm{v}_o(t) = 1-\exp\left(-\frac{t}{\mathcal{A}}\right), \tag{19}$$

$$\mathrm{v}_1(t) = -1+\frac{2t}{\mathcal{A}}\left(1-\mathrm{v}_o(t)\right)+\left(1-\mathrm{v}_o(t)\right)^2, \tag{20}$$

$$\begin{aligned}\mathrm{v}_2(t) &= 2+\left(1-\frac{2t}{\mathcal{A}}-\frac{2t^2}{\mathcal{A}^2}\right)\left(1-\mathrm{v}_o(t)\right)-2\left(1+\frac{2t}{\mathcal{A}}\right)\left(1-\mathrm{v}_o(t)\right)^2\\ &- \left(1-\mathrm{v}_o(t)\right)^3,\end{aligned} \tag{21}$$

$$\begin{aligned}\mathrm{v}_3(t) &= -5+\left(-4+\frac{2t}{\mathcal{A}}+\frac{4t^2}{\mathcal{A}^2}+\frac{4}{3}\frac{t^3}{\mathcal{A}^3}\right)\left(1-\mathrm{v}_o(t)\right)+4\left(1+\frac{3t}{\mathcal{A}}+\frac{2t^2}{\mathcal{A}^2}\right)\times\\ &\times \left(1-\mathrm{v}_o(t)\right)^2+2\left(2+\frac{3t}{\mathcal{A}}\right)\left(1-\mathrm{v}_o(t)\right)^3+\left(1-\mathrm{v}_o(t)\right)^4,\end{aligned} \tag{22}$$

$$\begin{aligned}\mathrm{v}_4(t) &= 14+\left(14-\frac{8t^2}{\mathcal{A}^2}-\frac{4t^3}{\mathcal{A}^3}-\frac{2}{3}\frac{t^4}{\mathcal{A}^4}\right)\left(1-\mathrm{v}_o(t)\right)-8\left(1+\frac{4t}{\mathcal{A}}+\frac{4t^2}{\mathcal{A}^2}+\frac{2t^3}{\mathcal{A}^3}\right)\times\\ &\times \left(1-\mathrm{v}_o(t)\right)^2-\left(13+\frac{30t}{\mathcal{A}}+\frac{18t^2}{\mathcal{A}^2}\right)\left(1-\mathrm{v}_o(t)\right)^3-2\left(3+\frac{4t}{\mathcal{A}}\right)\times\\ &\times \left(1-\mathrm{v}_o(t)\right)^4-\left(1-\mathrm{v}_o(t)\right)^5,\end{aligned} \tag{23}$$

and

$$\mathcal{A}=1+\frac{1}{2}\chi. \tag{24}$$

It should be important to note that the $\mathcal{O}(1)$ leading order term, v_o, is the solution of Eq.(16) for the case of null particle Reynolds number, $Re_s=0$, that is, the solution discussed in section 3.1. The non-linear effects are brought to the solution by the higher order terms in ε. The solution given in Eqs.(18) and (19)-(23) show the non-linear contribution related to Oseen correction for moderate values of $Re_s=\mathcal{O}(1)$.

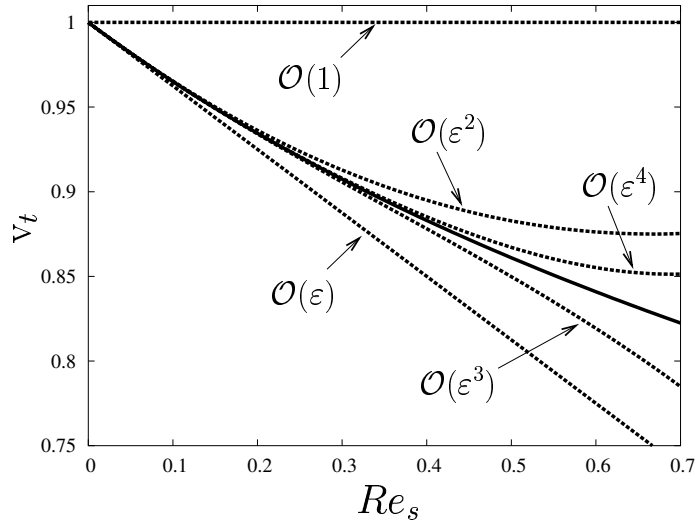

Figura 1: Terminal velocity of the particle as a function of Re_s. The solid line represents the predictions given by Eq.(26) and the dotted lines represent the asymptotic solutions expressed by Eq.(18), up to the order indicated on the figure.

In order to confirm this statement, the terminal velocity of the particle is examined as a function of the parameter Re_s. The terminal velocity of the particle can be determined analytically, since when the particle reaches the terminal velocity its acceleration vanishes. Then:

$$-\mathrm{v}_t - \frac{3}{8} Re_s \mathrm{v}_t^2 + 1 = 0, \tag{25}$$

where $\mathrm{v}_t = U_t/U_s$ denotes the terminal dimensionless velocity of the particle, and therefore:

$$\mathrm{v}_t = \frac{-8 + \sqrt{64 + 96 Re_s}}{6 Re_s} \tag{26}$$

Note that only the solution corresponding to $\mathrm{v}_t > 0$ in Eq.(26) is considered, and for $Re_s \to 0$ $\mathrm{v}_t \to 1$.

Figure (1) shows the results for the terminal velocity of the particle given by the asymptotic solution in Eq.(18) and Eq.(26), as a function of Re_s. The terminal velocity of the particle decreases as Re_s increases due to the increase of the total drag acting on the particle. Consequently, the resistance to the particle motion increase due to the presence of inertial effects in a regime of non-zero particle Reynolds number. The $\mathcal{O}(1)$ solution gives that the particle sediments with a terminal velocity independent of Re_s. This result is not verified by experimental observations for finite Reynolds numbers. As the higher order terms are considered in the asymptotic solution a better agreement of the particle terminal velocity is observed. The maximum value of Re_s for which a good agreement (with an error less than 2%) is still observed when comparing the $\mathcal{O}(\varepsilon^4)$ solution with Eq.(26) was $Re_s = 1/2$. It should be stressed that Oseen's correction is valid for $Re_s = \mathcal{O}(1)$ and if larger values of Re_s are used the Oseen approximation produces results physically inconsistent.

3.3. Linear equation with memory effects

In this case, the inertial non-linear drag in Eq.(12) is not considered. So, Eq.(12 reduces to the following integro-differential equation

$$\left(1 + \frac{1}{2}\chi\right) \frac{d\mathrm{v}}{dt} + \mathrm{v} + \sqrt{\frac{9\chi}{2\pi}} \int_o^t \left(\frac{d\mathrm{v}}{dt}\right)_{t=\zeta} \frac{1}{\sqrt{t-\zeta}} d\zeta - 1 = 0. \tag{27}$$

In order to solve the above equation we have used Laplace transform as defined in Abramowitz & Stegun (1965). For the initial condition $\mathrm{v}(0) = 0$, and using $\mathcal{A}$ as defined in Eq.(24) and $\mathcal{B} = (9\chi/2\pi)^{1/2}$ the following algebraic equation is obtained in terms of the Laplace transform of the particle velocity $\tilde{\mathrm{v}}$, namely

$$\mathcal{A} s \tilde{\mathrm{v}} + \tilde{\mathrm{v}} + \mathcal{B}\,(s\tilde{\mathrm{v}}) \left(\frac{\sqrt{\pi}}{\sqrt{s}}\right) - \frac{1}{s} = 0. \tag{28}$$

Solving equation (28) for $\tilde{\mathrm{v}}$ and making few algebraic manipulations, we obtain

$$\tilde{\mathrm{v}} = \frac{\mathcal{A}s + 1 - \mathcal{B}\sqrt{\pi s}}{s\left[(\mathcal{A}s+1)^2 - \mathcal{B}^2 \pi s\right]}. \tag{29}$$

Now, using inverse Laplace transform tables available in Abramowitz & Stegun (1965) and the software Maple 7 to perform this calculation, Eq.(29) is inverted to give the velocity of the particle as a function of time

$$\begin{aligned} \mathrm{v}(t) &= 1 + \mathcal{C}_1\Big(\exp(\mathcal{C}_2 t) - \exp(\mathcal{C}_3 t)\Big) - \exp(\mathcal{C}_4 t)\Big(\cosh(\mathcal{C}_5 t) + \mathcal{C}_6 \sinh(\mathcal{C}_5 t)\Big) \\ &+ \mathcal{C}_7 \mathrm{erf}(\mathcal{C}_8\sqrt{t})\exp(\mathcal{C}_9 t) - \mathcal{C}_{10}\mathrm{erf}(\mathcal{C}_{11}\sqrt{t})\exp(\mathcal{C}_{12} t), \end{aligned} \tag{30}$$

where erf is the error function and the coefficients $\mathcal{C}_1 \ldots \mathcal{C}_{12}$ are given as follows

$$\mathcal{C}_1 = \frac{\mathcal{A}}{\sqrt{-\mathcal{B}^2\pi(-\mathcal{B}^2\pi + 4\mathcal{A})}} \tag{31}$$

$$\mathcal{C}_2 = -\frac{2\mathcal{A} - \mathcal{B}^2\pi - \sqrt{\mathcal{B}^4\pi^2 - 4\mathcal{A}\mathcal{B}^2\pi}}{2\mathcal{A}^2} \tag{32}$$

$$\mathcal{C}_3 = -\frac{2\mathcal{A} - \mathcal{B}^2\pi + \sqrt{\mathcal{B}^4\pi^2 - 4\mathcal{A}\mathcal{B}^2\pi}}{2\mathcal{A}^2} \tag{33}$$

$$\mathcal{C}_4 = -\frac{2\mathcal{A} - \mathcal{B}^2\pi}{2\mathcal{A}^2} \tag{34}$$

$$\mathcal{C}_5 = \frac{\sqrt{\mathcal{B}^4\pi^2 - 4\mathcal{A}\mathcal{B}^2\pi}}{2\mathcal{A}^2} \tag{35}$$

$$\mathcal{C}_6 = \frac{2\mathcal{A} - \mathcal{B}^2\pi}{\sqrt{\mathcal{B}^4\pi^2 - 4\mathcal{A}\mathcal{B}^2\pi}} \tag{36}$$

$$\mathcal{C}_7 = \frac{2\mathcal{A}\mathcal{B}\sqrt{\pi}}{\sqrt{-4\mathcal{A} + 2\mathcal{B}^2\pi - 2\sqrt{-4\mathcal{A}\mathcal{B}^2\pi + \mathcal{B}^4\pi^2}}\sqrt{-4\mathcal{A}\mathcal{B}^2\pi + \mathcal{B}^4\pi^2}} \tag{37}$$

$$\mathcal{C}_8 = \frac{\sqrt{-4\mathcal{A} + 2\mathcal{B}^2\pi - 2\sqrt{-4\mathcal{A}\mathcal{B}^2\pi + \mathcal{B}^4\pi^2}}}{2\mathcal{A}} \tag{38}$$

$$\mathcal{C}_9 = \frac{\mathcal{B}^2\pi}{2\mathcal{A}^2} - \frac{1}{\mathcal{A}} - \frac{\sqrt{-4\mathcal{A}\mathcal{B}^2\pi + \mathcal{B}^4\pi^2}}{2\mathcal{A}^2} \tag{39}$$

$$\mathcal{C}_{10} = \frac{2\mathcal{A}\mathcal{B}\sqrt{\pi}}{\sqrt{-4\mathcal{A} + 2\mathcal{B}^2\pi + 2\sqrt{-4\mathcal{A}\mathcal{B}^2\pi + \mathcal{B}^4\pi^2}}\sqrt{-4\mathcal{A}\mathcal{B}^2\pi + \mathcal{B}^4\pi^2}} \tag{40}$$

$$\mathcal{C}_{11} = \frac{\sqrt{-4\mathcal{A} + 2\mathcal{B}^2\pi + 2\sqrt{-4\mathcal{A}\mathcal{B}^2\pi + \mathcal{B}^4\pi^2}}}{2\mathcal{A}} \tag{41}$$

$$\mathcal{C}_{12} = \frac{\mathcal{B}^2\pi}{2\mathcal{A}^2} - \frac{1}{\mathcal{A}} + \frac{\sqrt{-4\mathcal{A}\mathcal{B}^2\pi + \mathcal{B}^4\pi^2}}{2\mathcal{A}^2} \tag{42}$$

Despite the fact that we have found an analytical solution for Eq.(27), the error function which appears in its solution (30) needs to be calculated for complex arguments. This has restricted computations of this function based on the incomplete gamma function (eg. Press et al., 1992). The most appropriate way to deal with this issue has been to use the software Maple 7 for evaluating the error function and the large values this function may assume.

3.4. Non-linear equation with memory effects

This case corresponds to the particle motion governed by Eq.(12). In particular, this case does not admit an analytical solution. In order to solve the full integro-diferential equation Eq.(12) a fourth order Runge-Kutta scheme was implemented with a trapezoidal rule routine to perform the numerical integration of the convolution integral. Special care had to be taken in evaluating the memory integral because of the intense computational effort that is required. Even apparently small time steps used may produce a significant numerical uncertainty. As the kernel of the integral $(t-\zeta)^{-\frac{1}{2}}$ is singular at $\zeta = t$ it was necessary a singularity subtraction in order to perform the convolution integral at each time step. We follow closely the numerical procedures discussed in Press et al. (1992). By this way, we have performed calculation considering the coupling between the memory and the non-linear inertial forces on the particle motion.

The numerical solution of Eq.(12) was of considerable computational cost at moderate density ratio χ. It requires about 70 hours of CPU time for an integration over $100\tau_r$ that corresponds to a typical numerical computation in the presence of the memory contribution. The long processing time is a result of the small time step required for the convergence of the numerical solution. Typically, the time step used in the Runge-Kutta scheme coupled with the trapezoidal rule to solve the memory integral at each time has attended the following condition

$$\Delta t = \frac{1}{5}\min\left\{\chi, \frac{\chi}{Re_s}\right\}. \tag{43}$$

With this time we ensure that the position of the particle changed little in one time step. By the above numerical procedure we have performed computations for investigating the coupling between the memory force and the non-linear inertial force on the particle trajectory.

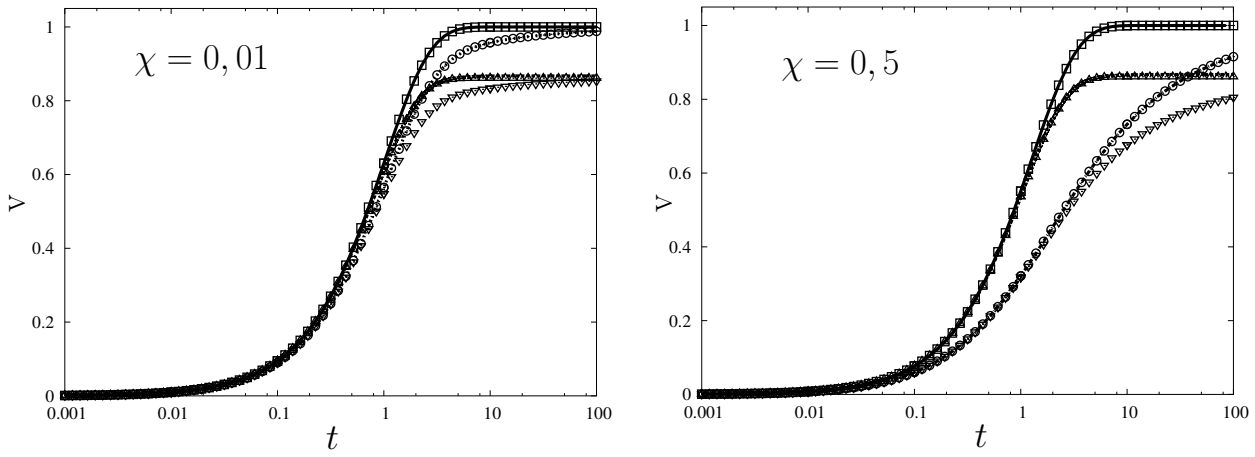

Figura 2: Time evolution of the particle velocity for $\chi = 1/100$ (left) and $\chi = 1/2$ (right). Soline line denotes the analytical solution of the linear problem without considering the memory effect and $\square$ represents the numerical solution; dashed line: analytical solution for the non-linear problem without memory effects for $Re_s = 1/2$, $\triangle$ numerical solution; dashed-dotted line: analytical solution of the linear problem with memory effects, $\odot$ numerical solution; $\bigtriangledown$ numerical solution of the non-linear problem with memory effects.

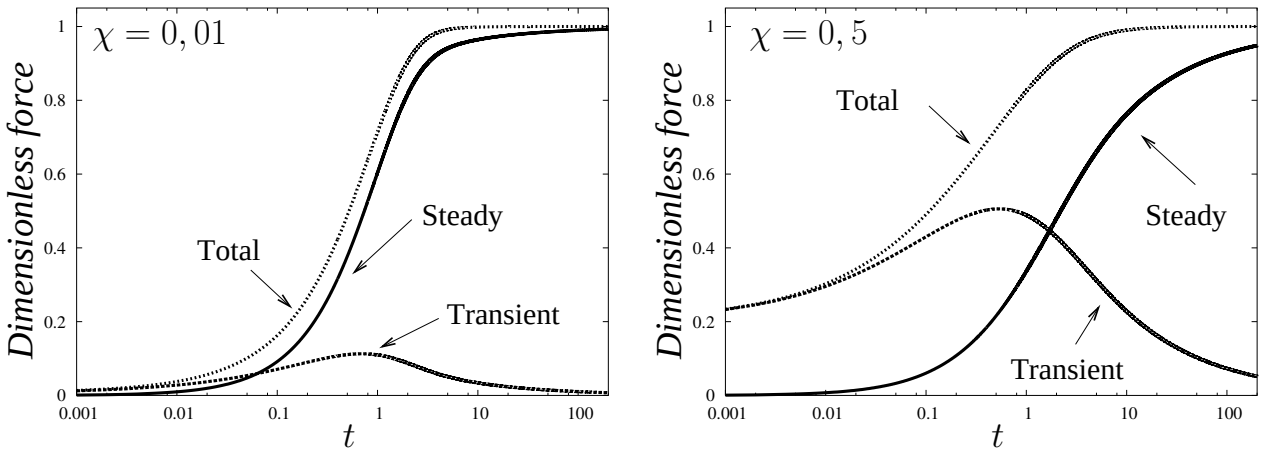

Figura 3: Time evolution of the hydrodynamic forces acting on the particle, for $\chi = 1/100$ (left) and for $\chi = 1/2$ (right). In both plots, $Re_s = 1/2$. The label "steady" identifies the linear viscous drag and the non-linear inertial drag, the label"transient" identifies the Basset memory drag and the virtual mass drag and the label "total" represents the total force acting on the particle.

4. Results and discussion

Once the velocity of the particle as a function of time was obtained, it is now possible to evaluate the time evolution of each hydrodynamic forces acting on the particle. We examine what the predominant forces are, during the motion of the particles for different conditions of Re_s and χ. As stated previously, a phenomenological analysis of the motion of the particle is important to guide the proposal of fluid-particle interaction forces that are needed in modelling particulate two-phase flows.

The first result to be analysed refers to the time evolution of the particle presented in Fig.(2) for $\chi = 1/100$ and $\chi = 1/2$. The values for χ were chosen in order to represent typical situations of fluid suspensions such as a gas-solid fluidized bed, in which $\chi \ll 1$, and a liquid-solid fluidized bed, where χ is typically $\mathcal{O}(1)$, say $1/2$. Based on the results presented in figs.(2), we can see that the numerical solution of Eq.(12) is in perfect agreement with the analytical solutions for the particular cases studied here. In addition, the results indicate that the transient diffusion of vorticity in the flow flow has an important influence on the motion of the particle, mainly on its evolution to the steady state at terminal velocity. This effect is noticeable for particles with density of the same order as that of the fluid, that is for $\chi \sim 1$. In this case, the time in which the particle reaches its terminal velocity may change from $\mathcal{O}(1)$ to $\mathcal{O}(100)$, depending if the effect of th memory force is considered or not on the particle trajectory. For $\chi \ll 1$, however, the time in which the terminal velocity is achieved is $\mathcal{O}(10)$.

In addition, the plots in Fig.(2) show that the contribution of the Oseen inertial drag, on the other hand, does not change the initial evolution of particle time development, independently whether the Basset drag was absent or not. At long times, however, the particle velocity is slightly changed so that the terminal velocity predicted by Eq.(26) is attained smoothly. Nevertheless, it should be important

to note that the asymptotic solution for the non-linear case with no memory effect reproduces the history of the particle velocity for times of the order of the particle relaxation time, but overestimates in approximately 2%, the value of the terminal velocity. It is seen that the time in which the terminal velocity is achieved when considering the non-linear drag is almost unaffected and it is comparable to those obtained in the linear cases. The resuls shown in Fig.(2) point out that the Basset force is responsible for the major changes on the time evolution of particle motion. That means that the flow memory, which is responsible for changing the mechanisms of a transient diffusion of vorticity causes a significant delay on its evolution. This mechanisms, nevertheless, does not change the terminal velocity of the particle that is predicted by the linear case governed by Eq.(14). The particle will reach its Stokes terminal velocity, though it will happen in a time scale that is much larger that the one predicted by Eq.(15). This time scale may even be of the order of the time required by the particle to go through all the sedimentation container, that is, a time scale $\mathcal{O}(L/U_s)$, with L denoting the length of the container. It is also seen that the relaxation time of the particle increases significantly as χ increases.

The total, transient and permanent hydrodynamic forces acting on the particles are presented in Fig.(3) for $\chi = 1/100$ and $\chi = 1/2$, and the isolated forces in Fig.(4). We can see that the transient forces are predominant on the early stages of the motion, specially for the case $\chi = 1/2$, presented in Fig.(3). In this case, both the virtual mass and the Basset drag are more important than the pseudo-steady viscous and inertial drags during the first period of the particle motion, such as shown in more details in Fig.(4). Similarly, when $\chi = 1/100$, a similar behaviour is observed, but is restricted to considerably smaller time intervals. In fact, the virtual mass unsteady drag is greater than the viscous Stokes drag during the first $3/500$ dimensionless times of the motion, whereas the Basset drag is important up to the $1/20$ dimensionless time. The analysis of the plots in figs.(3) and (4) suggest that the inertial transient have a neglected contribution in modelling suspensions of particles with much greater inertia than the fluid, that is $\chi \ll 1$ (e.g. dusty gas-suspension). In other words, one would say that the motion of particles in gas-solid suspensions is little influenced by any unsteady drag. This is related to the fact that the amount of kinetic energy of the particle motion used to accelerate the surrounding fluid is very small, and consequently these unsteady hydrodynamic drags decays very rapid compared with the particle relaxation time defined in Eq.(**??**).

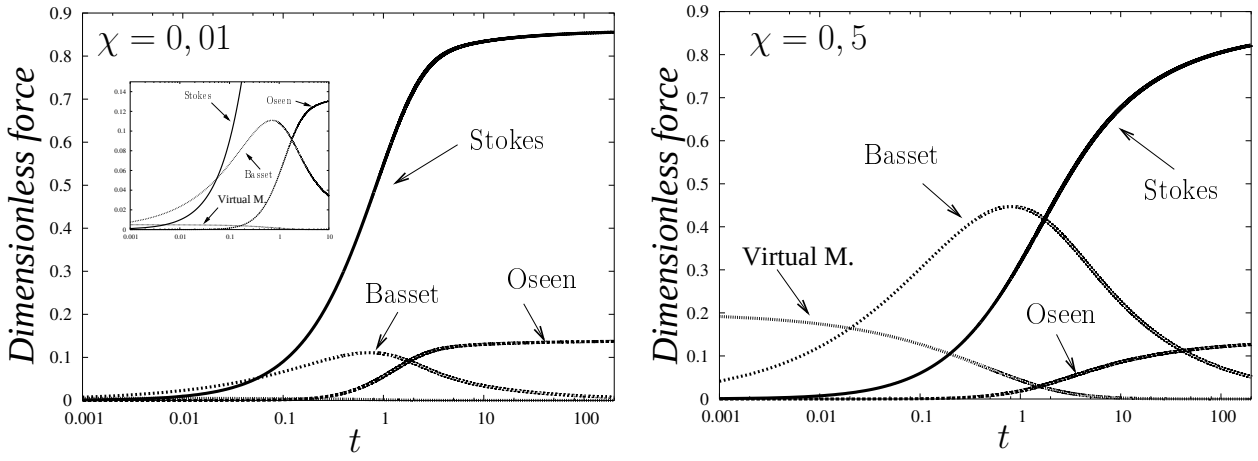

Figura 4: Time evolution of the forces acting on the particle for $\chi = 1/100$ (left) and for $\chi = 1/2$ (right). In both plots, $Re_s = 1/2$. The insert for $\chi = 1/100$ illustrates the early stages of the particle motion.

Fig.(4) for $\chi = 1/100$ also is showing that the virtual mass contribution is significant only during the first $1/10$ dimensionless times of the motion of the particle, and that it decays rapidly as the motion evolves. Note that at this time the Stokes drag is almost 10 times greater than this force. This result suggests that for small values of χ, the virtual mass unsteady force can be neglected with no major consequences to a accurate prediction of particle motion. In contrast, for $\chi = 1/2$ the virtual mass force has an important contribution during one relaxation time τ_r. These findings can also be inferred from the solution obtained in Eq.(15), plotted in Fig.(5). It is observed that for $\chi = 1/100$, the particle history is approximately the same as the one predicted when the virtual mass force is absent (i.e. when making $\chi = 0$ in Eq.(15)). On the other hand, the particle takes more time to reach the terminal velocity when $\chi = 1/2$, since it was retarded by the strong virtual mass force on the early stages of its motion.

Fig.(6) shows simulation results of the particle motion in the presence of the unsteady Basset drag and the Oseen drag contribution. As we can see the inertia on the wakes of the particles brought to the model by the Oseen drag does not affect significantly the time evolution of the Basset drag, the latter being reduced by about 15% on the interval between the first and 100 dimensionless times, for the case $\chi = 1/100$. It is also seen that for the case $\chi = 1/2$, this reduction was seen to persists for more than 100 dimensionless times. In addition, it is also observed that the intensity of the Basset drag was reduced by about 73% when χ was reduced by 50 times, confirming that the inertial unsteady forces loose importance as $\chi \to 0$. In particular, if on one hand the time when the maximum of the Basset force is reached is not sensitive to changes in χ, it is slightly influenced by the convective inertia. For $Re_s = 1/2$, the peak of the Basset drag is advanced by $1/10$ of dimensionless time, but still remains on the neighbourhood of $t = 1$. In fact, the time scale used to convert the dimensional variables of the problem into dimensionless variables, the particle relaxation time denotes the scale in which the Basset drag reaches its maximum. Therefore, it is observed that the Basset drag is a force that grows very rapidly, reaches its maximum on the neighbourhood of particle relaxation time and decays very slowly, as it can be seen on the logarithmic scale of

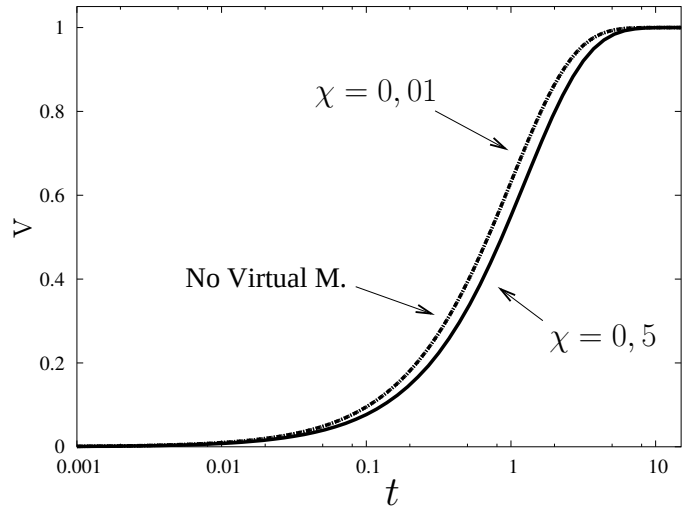

Figura 5: Influence of the virtual mass force on the motion of the particle predicted by Eq.(15), for $\chi = 1/100$ (dotted line) and $\chi = 1/2$ (solid line). The dashed line represents the motion of the particle when the virtual mass is absent.

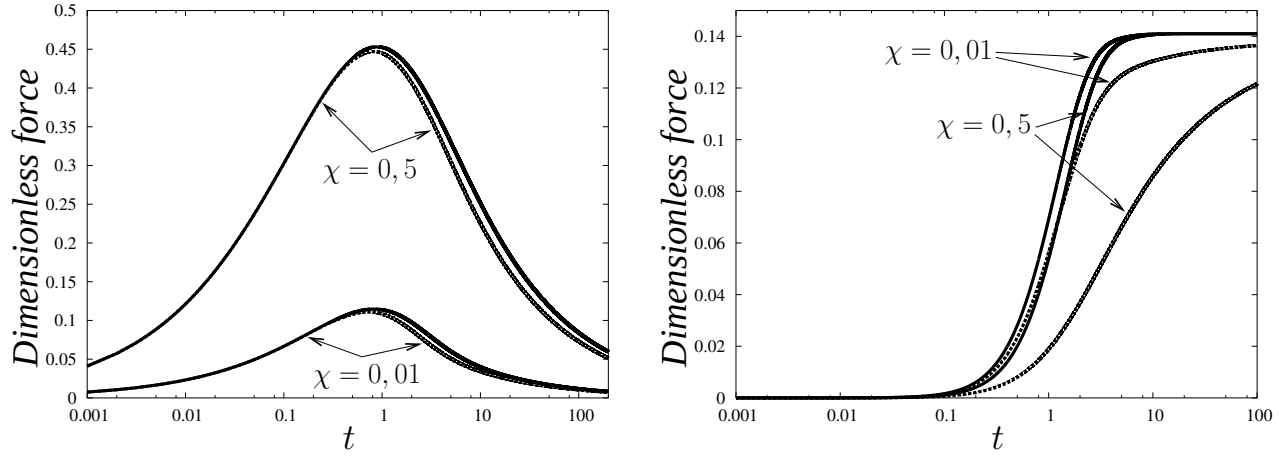

Figura 6: Left picture: Time evolution of the Basset drag for $\chi = 1/2$ and for $\chi = 1/100$. Solid lines represent the case with no Oseen drag and dotted lines represent the case with Oseen drag for $Re_s = 1/2$. Right picture: Evolution of the Oseen drag for $Re_s = 1/2$, for $\chi = 1/2$ and $\chi = 1/100$. Solid lines denote the case in the absence of Basset drag and dotted lined represent the case as Basset drag is considered.

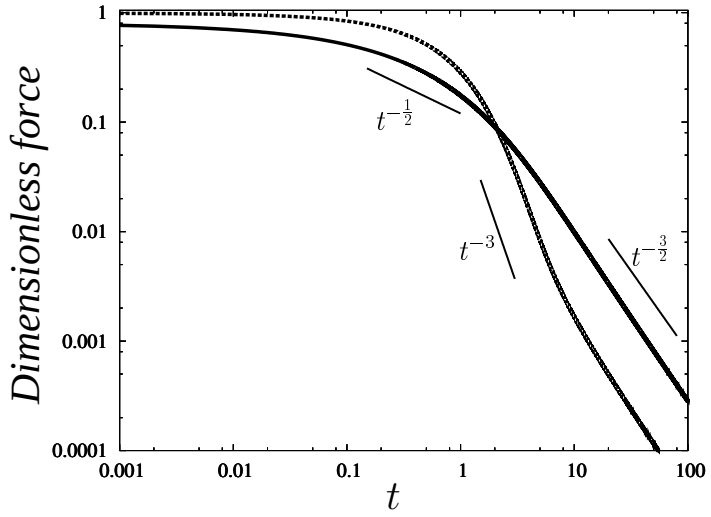

Figura 7: Evolution of the resultant force acting on the particle for $\chi = 1/100$ (dotted line) and for $\chi = 1/2$ (solid line) or $Re_s = 1/2$.

fig.(6)). This forces takes more than 100 dimensionless times to decay to the levels of intensity associated to the beginning of the motion (i.e. when $t \sim 10^{-3}$). For this reason, the omission of this force in modelling fluid-particle interactions in two-phase particulate flows where the inertia of the fluid is not negligible may lead to imprecise results on the prediction of the dynamics of the flow. Fig.(6) also presents the influence of the Basset drag on the evolution of the Oseen drag. An important delay on reaching the steady state can be observed. In particular, the unsteady diffusion of vorticity that occurs on the wakes of the particle for distances greater than the Oseen distance, i.e. $r > aRe_s^{-1}$, competes with the convective transport of vorticity in this region and it is responsible for reducing its intensity during three dimensionless times, for $\chi = 1/100$ and about ten dimensionless times for $\chi = 1/2$. This is directly related with the fact that the vorticity that is created on the particle surface and that is captured by the wake, is both convected by the flow on this region and diffused under the presence of inertial effects. In another words, the diffusive transport of vorticity is affected by the convective transport of vorticity in the region $r \sim aRe_s^{-1}$. Lovalenti & Brady (1993) and Lawrence & Mei (1993) have argued that the evolution of the particle to reach its terminal velocity changes its temporal decay from $t^{-\frac{1}{2}}$ to t^{-2} when convective effects are coupled to the unsteady memory diffusion effects in the description of the sedimentation of a particle starting from rest. More precisely, in Lovalenti & Brady (1993), and in its appendix D written by John Hinch, different time decays were predicted for several cases of arbitrary motion of a spherical particle.

Now, we turn to use scaling arguments in order to derive the time decay law for the total force acting on the particle for the present model. So, let us consider the equation of motion in its dimensional version, Eq.(11). A scale for the Basset drag is given by

$$\text{Basset} = 6a^2\sqrt{\pi\rho_f\mu_f}\int_o^{\hat{t}}\left(\frac{d\hat{\mathrm{v}}}{d\hat{t}}\right)_{\hat{t}=\zeta}\frac{1}{\sqrt{\hat{t}-\zeta}}d\zeta \sim a^2\sqrt{\rho_f\mu_f}\frac{U}{t^{\frac{1}{2}}}, \tag{44}$$

where U is a velocity scale and t is a characteristic time scale of the flow. In addition, a scale for the Oseen drag is found to be

$$\text{Oseen} = \frac{9}{4}\pi\rho_f a^2\hat{\mathrm{v}}^2 \sim \rho_f a^2 U^2. \tag{45}$$

We have identified three different steps in the transient motion of the particle. During the first step, when the particle is starting its motion, the important velocity scale is associated with vorticity diffusion, i.e. $U \sim \nu_f/a$, where ν_f is the kinematic viscosity μ_f/ρ_f. In this case, Eqs.(44) and (45) are re-written as:

$$\text{Basset} \sim a\rho_f^{-\frac{1}{2}}\mu_f^{\frac{3}{2}}\hat{t}^{-\frac{1}{2}} = \mathcal{O}(t^{-\frac{1}{2}}), \tag{46}$$

$$\text{Oseen} \sim \mu_f^2\rho_f^{-1} = \mathcal{O}(1). \tag{47}$$

Equations (46) and (47) indicate that at the early stages of the particle motion, Basset drag evolves temporally as $t^{-\frac{1}{2}}$, whereas the Oseen drag is $\mathcal{O}(1)$. This last statement is also shown in Fig.(3). The validity of these scales is restricted to the time interval defined at the beginning of the motion. That is, for $t \sim 0-1$ (or even $t \sim 0-10$, for $\chi = \mathcal{O}(1)$). The second part of the motion is observed for a time corresponding to the particle motion close to reach its terminal velocity. Under this condition the appropriate velocity scale is simply the convective particle velocity $a/\hat{t}$. With this scale, Eqs.(44) and (45) takes the form

$$\text{Basset} \sim a^3\rho_f^{\frac{1}{2}}\mu_f^{\frac{1}{2}}\hat{t}^{-\frac{3}{2}} = \mathcal{O}(t^{-\frac{3}{2}}), \tag{48}$$

$$\text{Oseen} \sim a^4\rho_f\hat{t}^{-2} = \mathcal{O}(t^{-2}). \tag{49}$$

Therefore, the Basset drag goes as $t^{-\frac{3}{2}}$ and the Oseen drag as t^{-2}. These scales seems to be valid for $t \sim 1-10$ (or for $t \sim 10-100$ when $\chi = \mathcal{O}(1)$). In the sequence, the third characteristic step of the particle particle motion occurs when it reachs its terminal velocity. In this case, it is clear that $U \sim U_t$. In this last part of the motion, both Basset and Oseen drags have the same temporal behaviour as presented in Eqs.(44) and (45).

The present analysis also can be used to predict the variations in the time decay evolution of the total force acting on the particle when an inertial convective drag is included in the model. Figure (7) shows the temporal decay of the resultant force acting on the particle for $\chi = 1/100$ and $\chi = 1/2$. We can see that for $\chi = 1/100$, the initial decay goes like t^{-3} between τ_r up to close to $10\tau_r$. This scale seems to be associated with the balance among the diverse power of temporal decays observed in the asymptotic solution of the equation of motion, Eq.(18), and the $\mathcal{O}(t^{-2})$ like decay of Oseens drag and, in a smaller influence, the $\mathcal{O}(t^{-\frac{1}{2}})$ of the Basset drag. After this interval, the decay of the total force goes like $t^{-\frac{3}{2}}$. In fact, if we analyze figs.(4) and (7) together, it can be inferred that the t^{-3} decay becomes more important as the Oseen drag passes to dominate the Basset drag, in the interval ranging from 2 to 10 dimensionless times. As time evolves, the transient effects of the flow dominate the time evolution towards the terminal velocity and the $t^{-\frac{3}{2}}$ behaviour, predicted by the scaling given in Eq.(48) is observed. The case $\chi \ll 1$, however, is not of major importance to evaluate the coupling between Basset drag and Oseen drag. When $\chi = 1/2$, on the other hand, the evolution towards the $t^{-\frac{3}{2}}$ decay is smooth, and a t^{-2} decay is not observed. This is due to the low values of the Oseen drag compared to the Basset drag for times up to $t = 50$ (see fig.(3)). Fig.(8), in contrast, shows the decay of the resultant force acting on a particle for different values of Re_s. It is seen that as Re_s increases, a stronger decay of the resultant force occurs after $t = 1$ in such a way that for $Re_s = 5$ and 10 a decay like t^{-2} clearly exists. For longer times, on the imminence of the steady state, the decay order returns to $t^{-\frac{3}{2}}$. This confirms that the non-linear inertial mechanisms on the flow do change the order of the temporal decay of the approach to the steady state. Due to the high computational cost to solve numerically Eq.(12) for large time intervals, it was not possible to explore the typical decay rates for very long times, predicted in Eqs. (44) and (45). We expect to investigate this long time behaviour based on an asymptotic solution of Eq.(12), what is currently under progress.

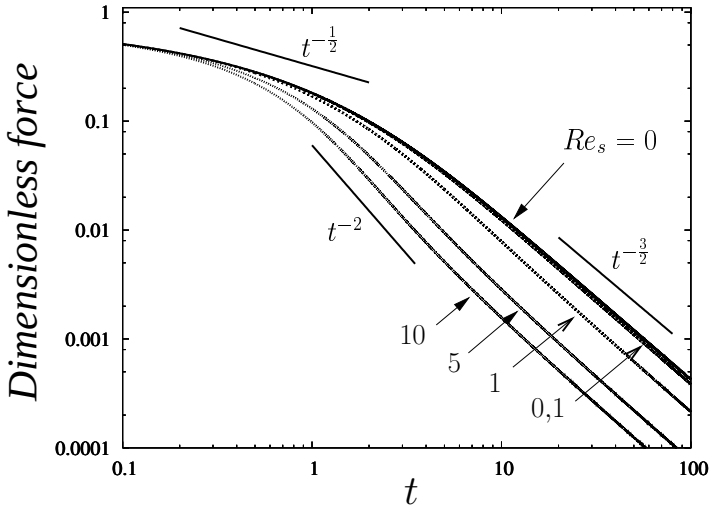

Figura 8: Evolution of the resultant force acting on the particle for $\chi = 1/2$ and for different values of Re_s.

Lawrence & Mei (1993) and, more recently Coimbra & Rangel (1998) have suggested that the form on the convolution kernel is changed when the inertial of the flow is considered. Formally, the $t^{-\frac{1}{2}}$-like kernel is valid only for $Re_s = 0$. In fact, Sano (1981) showed that the $Re_s \to 0$ limit is singular and, for that reason, there ought to be changes on the kernel of the memory integral. Lawrence & Mei (1993) used an asymptotic expression for the kernel that allowed them to get the predicted theoretical decay of the resultant force on the particle. Despite the results presented here were obtained considering the traditional kernel of the Basset drag, they have shown that the evolution towards the steady state of the motion changes with the presence of inertia. A final important finding of this work is presented in Fig.(8). It is seen that a faster evolution towards the steady state exists as Re_s increases. For $Re_s = 5$, the resultant force acting on the particle is approximately 10 times smaller than the value obtained for $Re_s = 1/10$ at t around 100 dimensionless times. Therefore, the our analysis was able to describe, at least, from a qualitatively point of view the faster evolution towards the terminal velocity of the particle when Re_s is not null.

5. Closing remarks

The study of the transient motion of a spherical particle developed in this work has provided insights that are important for modelling two-phase particulate systems. As discussed previously, the mechanisms of transient diffusion of vorticity brought up to the model by the Basset drag are of major importance on the description of the motion of particles whose inertia is comparable to the inertia of the fluid. In particulate systems in which the inertia of the fluid is considerably smaller than the inertia of the particles (i.e. typically

as occurs in gas solid-suspensions), the unsteady drags can be neglected with no relevant consequences to a correct prediction of the dynamics of these systems. However, the derivation of a model for particulate flows considering such effects is still an open problem and needs further research.

6. References

Abramowitz, M., Stegun, I.A., 1974, "Handbook of Mathematical Functions", *Dover Publications*, New York, USA.

Anderson, T. B. , Jackson, R., 1967, "A Fluid Mechanical Description of Fluidized Beds: Equations of Motion", *I&EC Fundamentals* Vol. 6, N^o 4, pp527-53 .

Basset, A. B., 1888, "A Treatise on Hydrodynamics", *Deighton Bell*, Cambridge, United Kingdom.

Batchelor, G. K., 1967, "An Introduction to Fluid Dynamics", *Cambridge University Press*, Cambridge, United Kingdom.

Coimbra, C. F. M., Rangel, R. H., 1998, "General Solution of the Particle Momentum Equation in Usteady Stokes Flow", *Journal of Fluid Mechanics*, vol. 370, pp53-72.

Kim, S., Karilla, S. J., 1991, "Microhydrodynamics: Principles and Selected Applications", *Butterworth-Heinemann*, Boston, USA.

Landau, L. D., Lifchitz, E., 1971, "Mécanique des Fluides", *Éditions MIR - Ellipses*, Poitiers, France.

Lawrence, C. J., Mei, R., 1995, "Long-Time Behavior of the Drag on a Body in Impulsive Motion", *Journal of Fluid Mechanics*, vol. 283, pp301-327.

Lovalenti, P. M., Brady, J. F., 1993, "The Hydrodynamic Force on a Rigid Particle Undergoing Arbitrary Time-Dependent Motion at Small Reynolds Number", *Journal of Fluid Mechanics*, vol. 256, pp561-605.

Press, W. H., Teukolsky, S. A., Vetterling, W. T., Flannery, B. P., 1992, "Numerical Recipes in Fortran 77" Second Edition, *Cambridge University Press*, Cambridge, United Kingdom.

Sano, T., 1981, "Unsteady Flow Past a Sphere at Low Reynolds Number", *Journal of Fluid Mechanics*, vol. 112, pp433-441.